

Aldehyde dehydrogenase activity of Wharton jelly mesenchymal stromal cells: isolation and characterization

Mehdi Najar · Emerence Crompt  · Leo A. van Grunsven · Laurent Dollé · Laurence Lagneaux

Received: 19 March 2018 / Accepted: 15 November 2018 / Published online: 4 January 2019
© Springer Nature B.V. 2019

Abstract Mesenchymal stromal cells (MSCs) are promising tools in regenerative medicine and targeted therapies. Although different origins have been described, there is still huge need to find a valuable source harboring specific subpopulations of MSCs with precise therapeutic functions. Here, we isolated by fluorescence activated cell sorting technique, two populations of Wharton's jelly (WJ)-MSCs based on their aldehyde dehydrogenase (ALDH) activity. Two different ALDH activities (low vs. high) were thus observed. We then analyzed their gene expression profile for stemness, phenotype, response to hypoxia, angiogenesis, hematopoietic support, immunomodulation and multilineage differentiation abilities (osteogenesis, adipogenesis, and chondrogenesis). According to ALDH activity, many differences in the mRNA expression of these populations were noticed. In conclusion, we provide evidences that WJ harbors two distinct populations of MSCs with


different ALDH activity. These populations seem to display specific functional competences that may be interesting for concise therapeutic applications.

Keywords Wharton jelly mesenchymal stromal cells · Aldehyde dehydrogenase activity · Fluorescence activated cell sorting · Transcriptome analysis

Introduction

Mesenchymal stromal cells (MSCs) are attractive therapeutic tools since their potential use in cellular immunotherapy and regenerative medicine (Forostyak et al. 2013; Dunavin et al. 2017; Zimmerlin et al. 2013). Finding therapeutic valuable sources of MSCs is a major concern for the field. Several sources have been thus reported such bone marrow (BM) (Najar et al. 2015), adipose tissue (AT) (Busser et al. 2015), foreskin (Najar et al. 2016a) and dental pulp (Kang et al. 2016) with contrasting results. Embryonic tissues like placenta (Lee et al. 2012) and umbilical cord (CB) (Rizk et al. 2017) seem to be important alternatives. The gelatin that surrounds the umbilical cord vessels called Wharton's jelly (WJ) is very promising; indeed, the WJ-MSCs have been discovered to be an ideal source of stromal cells (Beeravolu et al. 2017). Indeed, these cells have already presented high capacity to promote tissue regeneration and repair (Kamoliz et al.

Mehdi Najar and Emerence Crompt have contributed equally to this work.

M. Najar · E. Crompt  · L. Lagneaux
Laboratory of Clinical Cell Therapy, Jules Bordet
Institute, Université Libre de Bruxelles (ULB), Campus
Erasmé, Bâtiment de Transfusion (Level +1), Route de
Lennik no 808, 1070 Brussels, Belgium
e-mail: emerence.crompt@ulb.ac.be

L. A. van Grunsven · L. Dollé
Liver Cell Biology Laboratory, Vrije Universiteit Brussel,
Brussels, Belgium

2014) as well as demonstrated great immunotherapeutic features (Nagamura-Inoue and He 2014). Improving cell therapy implies also the research of specific populations with concise functional competences that may be interesting for targeted therapeutic applications. The aim of this work was to find a suitable method for isolating sub-populations of MSCs based on aldehyde dehydrogenase (ALDH) activity. Bodipy-aminoacetaldehyde (BAAA) contained in Aldefluor[®] assay (Storms et al. 1999; Alison et al. 2010) allows detecting cells with ALDH activity. ALDH enzymes were reported to have critical roles in cell protection, proliferation and differentiation (Balber 2011). The use of ALDH activity was thus referred as a reliable marker to isolate stem or progenitor cells (Ma and Allan 2011).

We first used fluorescence activated cell sorting (FACS) for isolating WJ-MSCs based on their ALDH activity (Herzenberg et al. 2002). Based on their ALDH activity, two populations of MSCs (referred as ALDH⁺ and ALDH⁻) were obtained and analyzed for their transcriptome. Accordingly, we noted several differences in their gene expression profile for stemness, cell cycle, immunomodulation, hypoxia response faculty, phenotype, hematopoietic support and multilineage capacities. Collectively, by selecting sub populations of WJ-MSCs with specific gene profile, we may improve cell therapy by delivering targeted therapeutic strategies.

Materials and methods

Ethics

This study was approved by the Bordet Institute Ethics Committee (Belgium) and conducted in accordance with the Declaration of Helsinki (1964). WJ samples were obtained following written informed consent from mothers (n = 4).

Isolation and culture of WJ-MSCs

The WJ were obtained after the full-term delivery and were directly processed. All the procedures for the isolation, culture and characterization of WJ were previously described (Najar et al. 2010a). Briefly, cords were transferred to an aseptic saline buffer, washed with HBSS (Lonza) and cut in small pieces.

The samples were sectioned longitudinally to expose the WJ on the surface and the matrix was completely immersed with Dulbecco's Modified Eagle's Medium with low glucose (Lonza: DMEM-LG) supplemented with 10% FBS (Sigma-Aldrich), 2 mmol/L L-glutamine and 50 U/mL penicillin/streptomycin (Lonza) during 15 days. Migratory and adhesive properties allow the WJs to exit and attach to the plastic surface. After this time, umbilical cord fragments were removed from the well to allow cell culture. When sub-confluence (80–90%) was achieved, adherent cells were harvested by TrypLE Select (Gibco, LifeTechnologies) and expanded until the desired passage.

Characterization of WJ-MSCs

The phenotype of MSCs was established by flow cytometry (MACSQuant[®], Miltenyi Biotec, Netherlands) using the following monoclonal antibodies: anti-CD45-FITC and anti-HLA-DR-PE (Exalpha Biologicals, Maynard, MA), anti-CD34-PE and anti-CD73-PE (BD Biosciences, San Diego, CA, USA), anti-CD14-PE, anti-CD19-PE, anti-CD105-FITC and anti-CD90-PE (R&D systems, Minneapolis, MN, USA). The trilineage potential of MSCs was confirmed through inducing differentiation into adipogenic, osteogenic and chondrogenic lineages using the appropriate culture conditions (NH media, Miltenyi Biotec).

Fluorescence activated cell sorting (FACS) analysis

Cell sorting was conducted using a FACS-Aria (BD Biosciences, San Jose, CA) as previously shown earlier (Mandelli et al. 1999). In summary, the instrument quality control was checked using Cytometer setting and tracking beads (CS&T) and software (FACSDiva) on a daily basis throughout this study. To analyze live cells and excluding debris as well as residual erythrocytes, two gates were respectively placed for scatter population and propidium iodide (PI) (Fluka, 70335). We also incorporated a doublet discriminating gate based upon height versus area of the side scatter signals. These settings were then adopted during the entire assay and the analysis was done using the Flo-Jo program (Tree Star, Ashland, www.flojo.com).

ALDH-positive and -negative cell population detection and sorting

The Aldefluor kit is used to isolate a population with high ALDH versus low ALDH enzymatic activity according to the manufacturer's instructions (Stem-Cell Technologies). Fluorescent ALDH substrate (BODIPY[®]—aminoacetaldehyde—BAAA/Aldefluor[®]) can be used to identify and isolate ALDH⁺ cells by flow cytometry according to our previous works (Dolle et al. 2012, 2015). Dissociated single cells (with trypsin) were suspended in Aldefluor assay buffer containing the BAAA (1 μ M per 3×10^6 cells) and incubated at + 37 °C without agitation during 50 min. BAAA (a non-polar fluorescent molecule) is taken up by viable cells through passive diffusion. The BAAA is composed of the bodipy molecule (which contains the green fluorescence) and the amino-acetaldehyde (which is the substrate for ALDH1A1). BAAA is metabolized by one of ALDH isoform (Moreb et al. 2012) to a carboxylate ion BAA[−] which is retained intracellularly. By becoming fluorescent, BAA-allows cells with high levels of ALDH to be isolated by FACS. The sorting gate of the ALDH⁺ cells was established using DEAB-treated cells as a reference. For all subsequent procedures, samples were constantly maintained at + 4 °C to prevent efflux. Aldefluor fluorescence was excited at 488 nm, and fluorescence emission was detected using a standard fluorescein-isothiocyanate 530/30 nm band-pass filter. All samples were thus sorted into 2 different collector tubes, namely “ALDH⁺” and “ALDH[−]”.

Gene expression analysis by Real Time PCR (qPCR)

After the sorting, the cells were directly spin-down by centrifugation. The extraction of the total mRNA was performed by mixing the cell lysate buffer [10 mL of BL-buffer from Promega (ref Z103c) with 10 μ L of thioglycerol (ref A208B)]. We used the RNeasy micro kit (ref 74004) from Qiagen to ensure optimal RNA purification because the number of cells obtained after the cell sorting was roughly small for some samples. The reverse transcription reaction was performed with 1 mg RNA using qScript cDNA SuperMix (Quanta Biosciences). Transcripts were quantified by qRT-PCR using 10 ng of cDNA, SYBR Green PCR Master Mix (Applied Biosystems, Lennik, Belgium) and

0.32 mM forward and reverse primers. The primers (Table 1) were designed thanks to ProbeFinder online software (Roche) or Primer Express 2.0 software (Applied Biosystems). The ABI Prism 7900 HT system (Applied Biosystems) was used to carry out the reactions and GAPDH gene used as a housekeeping gene to quantify and normalize the results. Dissociation curves were generated and the specificity of the PCR reactions was confirmed. The comparative $\Delta\Delta C_t$ method was finally used for the data analysis; data were normalized with the GAPDH genes to obtain the ΔC_t and were after calibrated with the geometric mean of the GAPDH ΔC_t to generate the $\Delta\Delta C_t$. Fold changes were then calculated as fold change = $2^{-\Delta\Delta C_t}$.

Statistical analysis

Data are presented as mean \pm standard error of the mean (SEM). The matched paired t test was used to compare the both sorted fractions. All analyses were performed with GraphPad Prism version 5.00 for windows (GraphPad Software, www.graphpad.com).

Results

ALDH activity dependent sorting and isolation of WJ-MSCs

Following the sorting, 2 populations with high and low ALDH enzymatic activity were thus isolated (ALDH⁺ and ALDH[−]). ALDH activity was significantly different in these 2 populations: 0.9 ± 0.04 UA for the ALDH[−] and 36.5 ± 1.36 UA for the ALDH⁺ population, $p = 0.0001$ (Fig. 1).

Gene expression profiling and analysis of ALDH sorted WJ-MSCs populations

Figure 2: Stemness (Nanog; Octamer-binding transcription factor 4(Oct4); Rex1)

Gene expression related to the stemness properties showed differences according to ALDH activity. We observed a significant increase in ALDH⁺ cells for the three targets compared to ALDH[−] population. We obtained in ALDH[−] cells an expression of 2788 ± 42.3 , 450.3 ± 19.7 , 215.8 ± 8.9 versus

Table 1 qRT-PCR primers

Transcripts	Forward	Reverse
<i>Cell cycle</i>		
p53	AGGCCTTGGAAGTCAAGGAT	CCCTTTTTGGACTTCAGGTG
p21	CGAAGTCAGTTCCTTGTGGAG	CATGGGTCTCTGACGGACAT
p16	TGCCTTTTCACTGTGTTGGA	TGCTTGTTCATGAAGTCGACAG
pRB	TCCTGAGGAGGACCCAGAG	AGGTCTTCTGTTTCTTCAAACCTCA
CDC25A	CGTCATGAGAACTACAAACCTTGA	TCTGGTCTCTTCAACACTGACC
FosB	CCGAGAGGAGACGCTCAC	CTGCTGCTAGTTTATTTTCGTTCC
STAT1	GACTGAGTTGATTTCTGTGTCTGAA	ACACCTCGTCAAACCTCCTCAG
CCNA	GGTACTGGAGTCCGGGAACC	GAAGATCCTTAAGGGGTGCAA
CCNB	CCTCCGGTGTCTGCTTC	TTCAGCATTAATTTTCGAGTTCC
CCNE	CTTCACAGGGAGACCTTTTAC	CATTGAGCCAGGACACAATAG
CDK1	TGGATCTGAAGAAATACTTGGATTCTA	CAATCCCCTGTAGGATTTGG
CDK2	GCTAGCAGACTTTGGACTAGCCAG	AGTCTCGGTACCACAGGGTCA
<i>Hypoxia</i>		
HIF1 α	TGGAATGGAGCAAAAAGACAA	CAGCTGTGGTAATCCACTTTCA
HIF2 α	CATCATGCGACTGGCAAT	GCTTCGGACTCGTTTCAGA
GLUT1	CTTCCTACCCAACCACTCAAA	CCCTCTCCTCCCTGCACT
<i>Stemness</i>		
SOX2	CCATCCACACTCACGCAAAA	CCCCCAAAAAGAAGTCCCAA
REX1	CCCTGGACTGCGAGATGT	AGGCTTCACGAAGGTGTGTCAT
NANOG	ACAACTGGCCGAAGAATAGCA	GGTCCCAGTCGGGTTCAC
OCT4	CTTCGCAAGCCCTCATTTAC	TTGATGTCCTGGGACTCCTCC
<i>Angiogenesis</i>		
ANG1	TTCCTGTCAAGTCATCTTGTGAA	TTTTATTAAGGTTGCACATCCAAG
ANG2	GGCAGCGTTGATTTTCAGAG	TTGCGAAACAAACTCATTTCC
FLT1	ACATTGGCCACCATCTGAAC	GCAGTATTCAACAATCACCATCA
VEGF	CTACCTCCACCATGCCAAGT	GCAGTAGCTGCGCTGATAGA
<i>Phenotype</i>		
CD54	AGTGATCAGGGTCCTGCAA	GGGAGGGAGTCTCTCCAATAC
CD58	CCAATGCATGATACCAGAGCAT	CCAATGCATGATACCAGAGCAT
CD106	GGCTGTGAATCCCCATCTT	AATTGGTCCCCTCACTCCTC
CD146	GGGTACCCCATTCCTCAAGT	CAGTCTGGGACGACTGAATG
CD200	TCTACCTACAGCCTGGTTTGG	TGGGTCACCACTTGCACTT
<i>Immuno</i>		
GAL1	AAGCTGCCAGATGGATACGAA	CGTCAGCTGCCATGTAGTTGA
COX1	CCTGCAGCTGAAATTTGACCCA	ACCTTGAAGGAGTCAGGCATG
COX2	GCTCAAAACATGATGTTTGCATTC	GCTGGCCCTCGCTTATGA
HGF	CAATGCCCTCTGGTTCCCTT	AGGCAAAAAGCTGTGTTTCGTG
LIF	TGAAAACCTGCCGGCATCTGA	CTGTGTACTGCCGCAAGA
<i>Hematopoiesis</i>		
IL-6	AAATTCCGGTACATCCTCGACGG	GGAAGGTTTCAGGTTGTTTTCTGC
IL-8	CTGTAAATCTGGCAACCCTAGTCT	CAAGGCACAGTGGAAACAAGGA
SCF	AGCCAGCTCCCTTAGGAATG	CGAGTGGGTCTAGCGGAAAG
MMP2	TGATCTTGACCAGAATACCATCGA	GGCTTGCGAGGGAAGAAGTT
SDF1	CTGTGCCCTTCAGATTGTAGCC	CTGTAAGGGTTCTCAGGCG

Table 1 continued

Transcripts	Forward	Reverse
<i>Osteogenesis</i>		
OSX	TAGGCAGCAGCAGTAGCAGA	TCTGACTCCAGAGTCCTTGCT
BSP	TACACGGGCGTCAATGAATA	AGGTTCCTTCCTCACTTT
RUNX2	TTACTTACACCCCGCCAGTC	TATGGAGTGCTGCTGGTCTG
OPN	TTGCAGTGATTTGCTTTTGC	GCCACAGCATCTGGGTATTT
OPG	GGCAACACAGCTCACAAGAA	CGCTGTTTTTCACAGAGGTCA
<i>Adipogenesis</i>		
AdipoQ	GCTCTGTGCTCCTGCATCTG	GAGTCCATTACGCTCTCCTCC
PPAR γ	CACAAGAACAGATCCAGTGGTTGCAG	AATAATAAGGTGGAGATGCAGGCTCC
KLF2	CATCTGAAGGCGCATCTG	CGTGTGCTTTCCGGTAGTGG
KLF5	GGCTTTACTCAAGCAGATCTCATC	CCCTACCCATGTTGAGACG
CEBP δ	TGACAGCCTCGCTTGGACG	CTCTCGTCGTCGTACATGGC
CEBP α	TATAGGCTGGGCTTCCCCTT	AGCTTTCTGGTGTGACTCGG
<i>Chondrogenesis</i>		
COL2 α 1	CCCATCTGCCCAACTGACC	CCAGTCCGTCCTCTTTACCC
ACAN	GTGAGGAGGACATCACCGTC	AAGGCAGTGGCCCCCTATTTC
SOX9	GTACCCGACACTTGACACAAC	TCGCTCTCGTTTCAAGAAGTCTC
COMP	CAGGGAGATCACGTTCTCTGA	GGCCGGTGCGTACTGAC
<i>Housekeeping</i>		
GAPDH	AATCCCATCACCATCTTCCA	TGGACTCCACGACGTACTCA

5184 \pm 364.3, 1272 \pm 57.7, 354.9 \pm 14.15 in ALDH⁺ cells for Rex1, Nanog and Oct4 respectively ($p = 0.0084$, $p = 0.0018$, $p = 0.0014$) (Fig. 2).

Figure 3: Proliferation/cell cycle (*CyclinA (CCNA)*, *CCNB*, *CCNE*; *CDK1*, *CDK2*, *Fos proto-oncogene (Fosb)*; *p21*; *p53*; *p16*; *retinoblastoma protein (pRB)*; *cell division cycle 25A (CDC25A)*; *signal transducer and activator of transcription (STAT1)*)

Distinct gene expressions concerning proliferation and cell cycle were observed in both populations according to ALDH activity. We observed a significant increase in ALDH⁺ cells for all the targets compared to ALDH⁻ population. About the cycline dependent kinase inhibitors, we obtained in ALDH⁻ cells an expression of 21,491 \pm 325, 105,959 \pm 5793, 15,335 \pm 638.3, versus 73,235 \pm 4697, 152,135 \pm 4209, 32,872 \pm 1555 in ALDH⁺ cells for p16, p21 and p53 respectively ($p = 0.0014$, $p = 0.0075$, $p = 0.0034$). We also noted increased expressions for two cyclin

dependent kinase CDK1 and CDK2 with significant p value (19,271 \pm 396.5, 1810 \pm 129 versus 23,174 \pm 1078, 4033 \pm 334.8). The mRNA of FosB in WJ-MSCs was 2933 \pm 165 in ALDH⁻ and 8141 \pm 546.6 in ALDH⁺ cells ($p = 0.0029$). CCNA, CCNB and CCNE presented same profile with 1086 \pm 27.86, 182.2 \pm 13.92, 867.5 \pm 34.83 versus 1478 \pm 63.8, 287.7 \pm 8.84, 1381 \pm 75.4 ($p = 0.0023$, $p = 0.0007$, $p = 0.0065$). Finally, PrB, Stat1 and CDC25A were also more expressed in ALDH⁺ cells compared to ALDH⁻ cells with significant p values ($p = 0.0410$, $p = 0.0053$, $p = 0.0002$) (Fig. 3).

Figure 4: Phenotype (melanoma cell adhesion molecule CD146 (MCAM); CD200; vascular cell adhesion molecule 1 CD106 (VCAM-1); intercellular adhesion molecule 1 CD54 (ICAM-1); CD58 (LFA-3))

The genes related to the phenotype of MSCs significantly differed between ALDH⁺ and ALDH⁻ subsets of WJ-MSCs. CD146 was the most expressed with

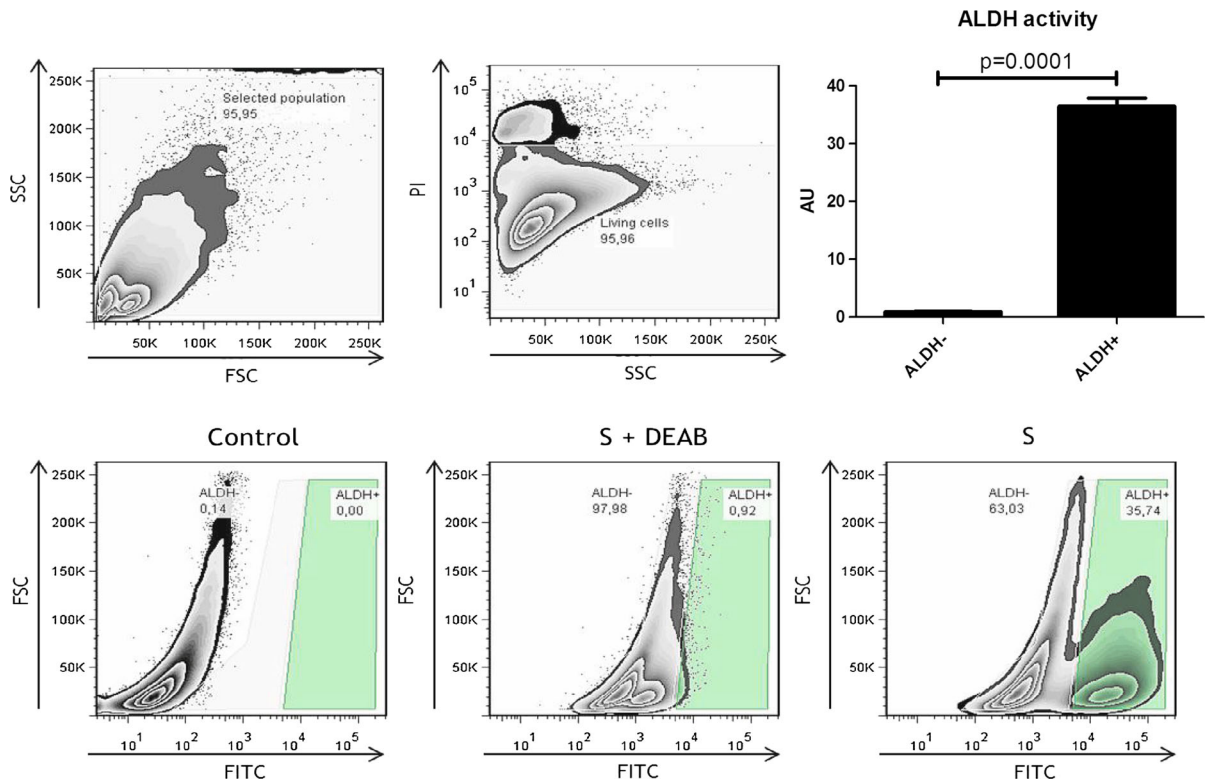


Fig. 1 Identification and sorting of WJ-MSCs based on ALDH activity. Representative pictures showing the flow cytometry profile of ALDH⁺ and ALDH⁻ populations of WJ-MSCs based

on their respective ALDH activity. ALDH activity within WJ-MSCs are reported as the mean \pm SEM (Arbitrary unit) (S for substrate)

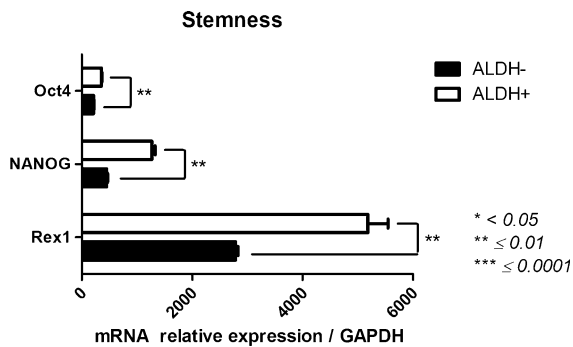


Fig. 2 Stemness profile of ALDH⁺ and ALDH⁻ WJ-MSCs. After sorting ALDH⁺ and ALDH⁻ WJ-MSCs by FACS technique, we determined by qPCR their expression of *Oct4*, *Nanog* and *Rex1* as description of their stemness. Data are presented as mean \pm SEM of mRNA gene expression relative to *GAPDH* expression

$62,344 \pm 4217$ in ALDH⁺ cells and $30,557 \pm 1987$ in ALDH⁻ cells ($p = 0.0133$). CD54, CD58 and CD106 presented the same profile with significant p values ($p = 0.0044$, $p = 0.0009$, $p = 0.0014$).

CD200 was less expressed in ALDH⁻ population ($23,065 \pm 2233$ vs. $42,478 \pm 2082$, $p = 0.0108$) (Fig. 4).

Figure 5: Hypoxia response (hypoxia-inducible factor (HIF)-1 α ; HIF-2 α ; Solute carrier family 2 member 1 (GLUT1))

Hypoxia responses genes were distinctively expressed between both ALDH populations. We clearly observed three significant increases for HIF1 α , HIF2 α and GLUT1 in ALDH⁺ cells ($p = 0.0174$, $p = 0.0016$, $p = 0.0043$). We noticed that GLUT1 was the most expressed with mean of $55,813 \pm 4288$ in ALDH⁻ population versus $80,907 \pm 2631$ in ALDH⁺ cells (Fig. 5).

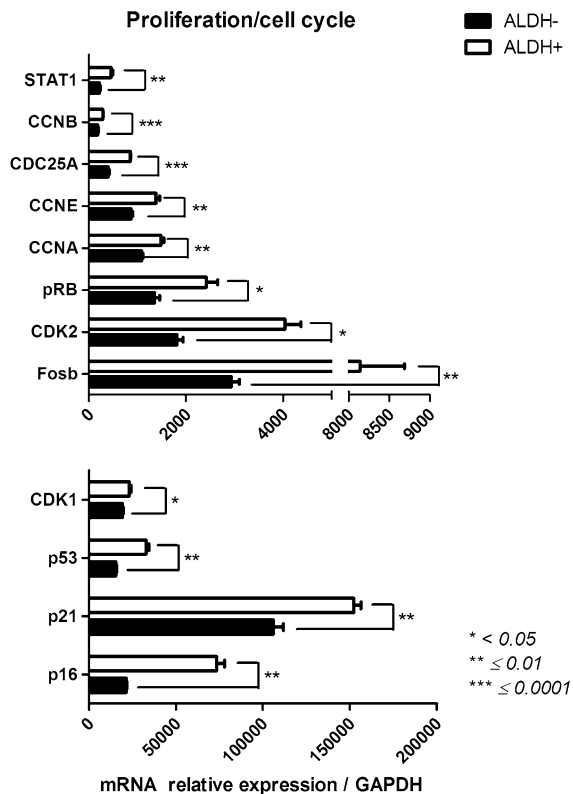


Fig. 3 Proliferation and cell cycle profile of ALDH⁺ and ALDH⁻ WJ-MSCs. After sorting ALDH⁺ and ALDH⁻ WJ-MSCs by FACS technique, we evaluated by qPCR their expression of *FosB*, *CDK1*, *CDK2*, *Cyclin A*, *Cyclin B*, *Cyclin E*, *p16*, *p21*, *p53*, *pRB* and *STAT1* as indication of their proliferation and cell cycle. Data are presented as mean \pm SEM of mRNA gene expression relative to *GAPDH* expression

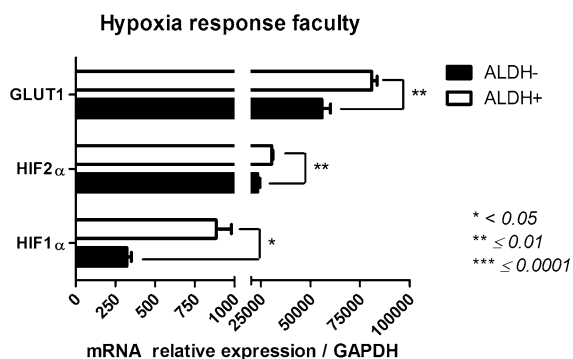


Fig. 4 Hypoxia response faculty of ALDH⁺ and ALDH⁻ WJ-MSCs. After sorting ALDH⁺ and ALDH⁻ WJ-MSCs by FACS technique, we investigated by qPCR their expression of *HIF-1α*, *HIF-2α*, *Glut1* as proof of their hypoxia response faculty. Data are presented as mean \pm SEM of mRNA gene expression relative to *GAPDH* expression

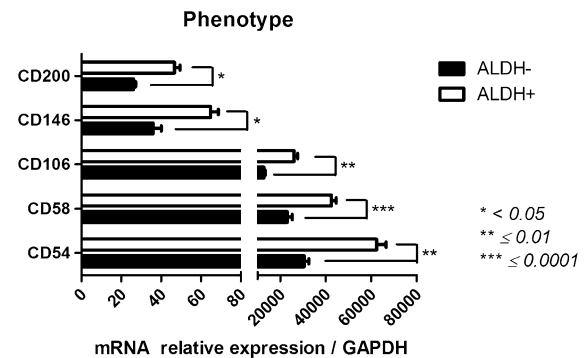


Fig. 5 Phenotype of ALDH⁺ and ALDH⁻ WJ-MSCs. After sorting ALDH⁺ and ALDH⁻ WJ-MSCs by FACS technique, we assessed by qPCR their expression of *CD146*, *CD200*, *CD106*, *CD54*, and *CD58* as characterization of their phenotype. Data are presented as mean \pm SEM of mRNA gene expression relative to *GAPDH* expression

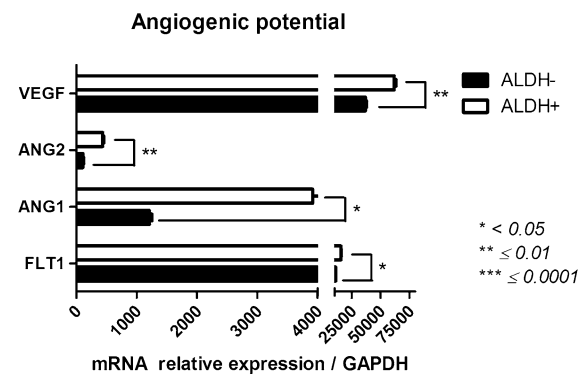


Fig. 6 Angiogenic potential of ALDH⁺ and ALDH⁻ WJ-MSCs. After sorting ALDH⁺ and ALDH⁻ WJ-MSCs by FACS technique, we studied by qPCR their expression of *ANG1*, *ANG2*, *FLT1* and *VEGF*, as evidence of their angiogenic potential. Data are presented as mean \pm SEM of mRNA gene expression relative to *GAPDH* expression

Figure 6: Angiogenesis (angiopoietin (ANG)1, ANG2, Fms related tyrosine kinase 1 (FLT1); vascular endothelial growth factor (VEGF))

Relevant differences between ALDH⁺ and ALDH⁻ populations were noted for genes associated with angiogenesis faculty of WJ-MSCs. All the envisaged targets were less expressed in ALDH⁻ cells with mean expression of 1211 ± 41.5 , 112 ± 8.1 , $36,732 \pm 918$, $11,045 \pm 98.8$ compared with 3919 ± 250.4 , 439.5 ± 16.5 , $61,899 \pm 1520$, $15,593 \pm 398.5$ in ALDH⁺ cells for *ANG1*, *ANG2*, *FLT1*, *VEGF* respectively ($p = 0.0022$, $p = 0.0006$, $p = 0.0014$, $p = 0.0002$) (Fig. 6).

Figure 7: Hematopoietic support (matrix metalloproteinase 2 (MMP2); stromal derived factor 1 (SDF1); kit ligand (SCF); interleukin-6 (IL-6); IL-8)

Based on their ALDH activity, ALDH populations of WJ-MSCs presented distinct expressions of genes for hematopoiesis. ALDH⁺ cells presented higher expression of IL6 and IL8 mRNA with respectively $450,699 \pm 5136$ and $75,812 \pm 6415$ compared to $247,255 \pm 5268$, $44,240 \pm 2001$ in ALDH⁻ cells ($p < 0.0001$, $p = 0.0065$). MMP2, SDF1, and SCF presented the same profile ($261,792 \pm 9868$, 528.1 ± 12.2 , $16,442 \pm 857.9$ in ALDH⁻ cells versus $319,505 \pm 7234$, 660.8 ± 12 , $25,809 \pm 977.1$ in ALDH⁺ cells) (Fig. 7).

Figure 8: Immunomodulation (Galectin1 (GAL1); hepatocyte growth factor (HGF); leukemia inhibitory factor (LIF); cytochrome c oxidase subunit 1 (COX1), COX2)

Differences within WJ-MSCs immunoregulatory genes are dependent on ALDH activity. All the studied genes were most expressed in ALDH⁺ cells compared to ALDH⁻ cells. GAL1 was the most expressed in WJ-MSC ALDH⁺ cells with $831,814 \pm 42,045$ compared to ALDH⁻ $1,294,000 \pm 38,276$ ($p = 0.0034$). COX1 and COX2 were also significantly upregulated in ALDH⁺ cells (354.4 ± 35 , $147,693 \pm 2878$ versus 854.7 ± 13.65 , $218,235 \pm 10,349$,

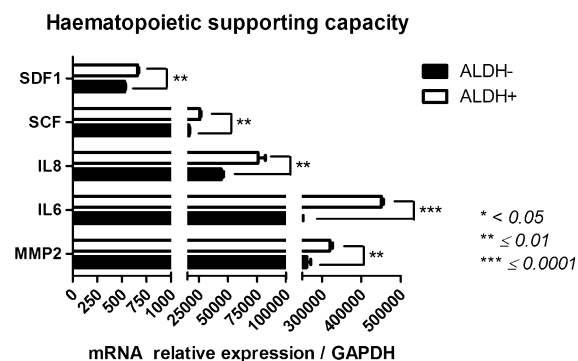


Fig. 7 Hematopoietic supporting capacity of ALDH⁺ and ALDH⁻ WJMSCs. After sorting ALDH⁺ and ALDH⁻ WJ-MSCs by FACS technique, we analyzed by qPCR their expression of MMP2, SDF1, SCF, IL-6 and IL-8 as illustration of their hematopoietic supporting capacity. Data are presented as mean ± SEM of mRNA gene expression relative to GAPDH expression

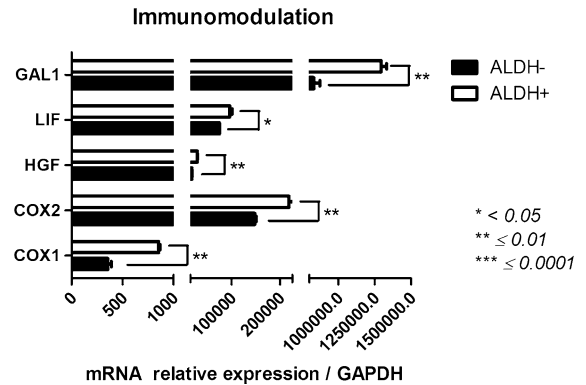


Fig. 8 Immunomodulatory ability of ALDH⁺ and ALDH⁻ WJ-MSCs. After sorting ALDH⁺ and ALDH⁻ WJ-MSCs by FACS technique, we examined by qPCR their expression of GAL1, HGF, LIF, COX1 and COX2 as demonstration of their immunomodulatory ability. Data are presented as mean ± SEM of mRNA gene expression relative to GAPDH expression

respectively). LIF and HGF presented the same profile with less expression in ALDH⁻ population ($p = 0.0277$, $p = 0.0025$) (Fig. 8).

Trilineage potential (Fig. 9)

The gene expression illustrating the differentiation into either adipogenic, osteogenic or chondrogenic lineages was contrasting according to ALDH activity of both WJ-MSCs populations.

Adipogenesis potential (CCAAT/enhancer binding protein alpha (C/EBP- α), C/EBP- δ ; Peroxisome proliferator activated receptor gamma (PPAR- γ); Kruppel like factor (KLF2); KLF5; Adiponectin (ADIPOQ)) The selection of the ALDH⁺ and ALDH⁻ populations made possible to isolate cell populations displaying different levels of C/EBP- α with a greater gene expression for the ALDH⁺ subset. The levels of C/EBP- α was 551.2 ± 13 for ALDH⁺ cells versus 305 ± 22.3 for ALDH⁻ subset ($p = 0.0017$). Concerning C/EBP- δ gene expression, the ALDH⁺ population showed the higher rate (886.9 ± 42.6) compared to the ALDH⁻ population (299.8 ± 5.8) ($p = 0.0008$). Moreover, the levels of KLF2 and KLF5 were also upregulated in ALDH⁺ compared to ALDH⁻ populations (2680 ± 167.3 vs. 3681 ± 91.7 for KLF2) (146.4 ± 8.5 vs. 237.8 ± 6.1 for KLF5) ($p = 0.0095/p = 0.0003$). However, PPAR γ and ADIPOQ were not significantly different (Fig. 9a).

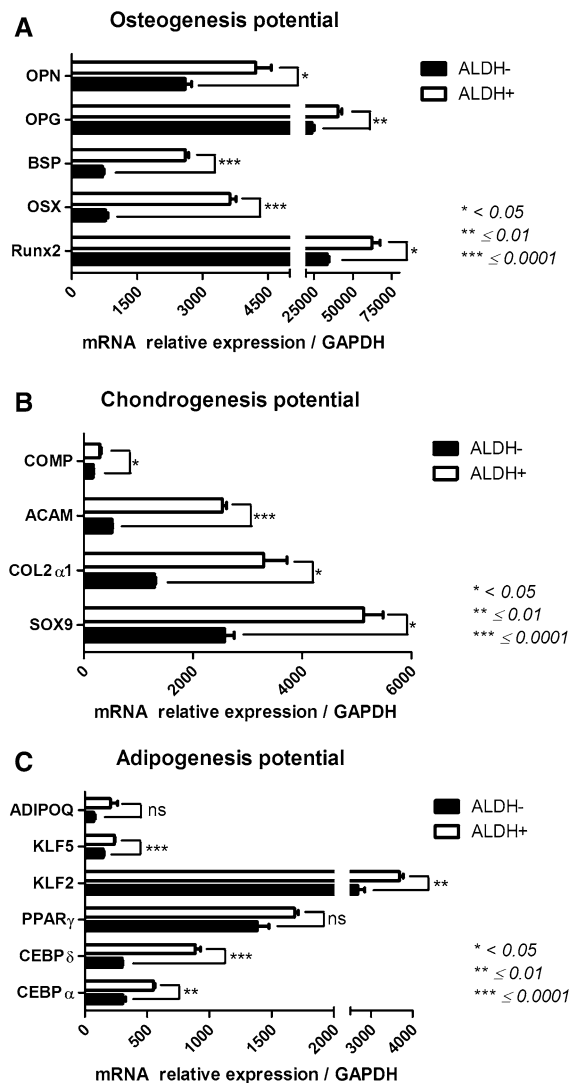


Fig. 9 Osteogenic competence of ALDH⁺ and ALDH⁻ WJ-MSCs. After sorting ALDH⁺ and ALDH⁻ WJ-MSCs by FACS technique, we explored by qPCR their expression of *Runx2*, *OSX*, *BSP*, *OPG* and *OPN* markers as manifestation of their aptitude to differentiate towards the osteogenic lineage (a). Concerning the chondrogenic competence of ALDH⁺ and ALDH⁻ WJ-MSCs, we checked the expression of *Sox9*, *Col2a1*, *ACAN* and *COMP* as reflection of their aptitude to differentiate towards the chondrogenic lineages (b). The adipogenic competence of ALDH⁺ and ALDH⁻ WJ-MSCs was analyzed and the expression of *C/EBP- α* , *C/EBP- δ* , *PPAR- γ* , *KLF2*, *KLF5* and *ADIPOQ* markers was evaluated as confirmation of their aptitude to differentiate towards the adipogenic lineages (c). Data are presented as mean \pm SEM of mRNA gene expression relative to GAPDH expression

Osteogenesis potential (*Runt related transcription factor 2* (*Runx2*); *Osterix* (*OSX*); *Integrin binding sialoprotein* (*BSP*); *TNF receptor superfamily*

member 11 (*OPG*); *Secreted phosphoprotein type 1* (*OPN*)) The ALDH⁺ population significantly showed the highest gene expression in ALDH⁺ cells for *Runx2* ($62,377 \pm 5206$), *BSP* (2606 ± 71.8), *OPG* ($40,426 \pm 2441$) and *OPN* (4222 ± 359) genes compared to the ALDH⁻ population (*Runx2*: $33,603 \pm 1211$, $p = 0.0102$; *BSP*: 706.5 ± 30.1 , $p = 0.0003$; *OPG*: $23,858 \pm 1419$, $p = 0.0094$; *OPN*: 2600 ± 149.5 , $p = 0.0104$) (Fig. 9b).

Chondrogenesis potential (*Sry box 9* (*Sox9*); *Collagen type II alpha 1 chain* (*Col2a1*); *Aggrecan* (*ACAN*); *Cartilage Oligomeric matrix protein* (*COMP*)) ALDH⁻ and ALDH⁺ cells showed significant different expression of *Sox9* (2578 ± 178.2 and 5128 ± 354.9 respectively, $p = 0.0111$). Concerning *Col2a1* expression, the lowest expression was seen in the ALDH⁻ population (1299 ± 21.9) in comparison to the ALDH⁺ population (3295 ± 428.1 , $p = 0.018$). For *ACAN* and *COMP* expressions, ALDH⁺ population showed a higher expression than its negative counterpart ($p = 0.0001$ and $p = 0.0293$ respectively) (Fig. 9c).

Discussion

Their self-renewal, multilineage differentiation capacity and immunomodulatory abilities make mesenchymal stromal cells (MSCs) promising tools for different therapeutic applications. According to their origin, MSCs may share some characteristics (Hoogduijn et al. 2010) but may also present functional differences related to distinct gene and protein profiles (Busser et al. 2015; Fayyad-Kazan et al. 2017). The umbilical cord is becoming an important alternative source of MSCs (Davies et al. 2017). Wharton's jelly gelatin, firstly considered as a waste product, is currently fast obtained, non-invasive and abundant source of MSCs (Najar et al. 2016a; Beeravolu et al. 2017; Boey et al. 2017). Moreover this source already demonstrated benefic effects in cardio-regenerative medicine, in diabetes treatment or also in modulating Graft Versus Host Disease (Kamoloz et al. 2014). Understanding the product profile of the intended therapy is crucial to guarantee a safe therapeutic use of MSCs (Sharpe et al. 2012; Atouf et al. 2013; De Kock et al. 2012). No marker is currently available for identifying MSCs from various tissue environments with distinct

competences to provide targeted efficient therapeutic (Najar et al. 2010a).

Aldehyde dehydrogenase (ALDH) activity was shown to be important in stem cell physiology (Ma and Allan 2011) and for tissue repair and regeneration (Kusuma et al. 2016; Kusuma et al. 2017; Sherman et al. 2017). Moreover, the activity and expression of ALDH seem to be a promising marker and potential therapeutic target for treating several malignancies (Rodriguez-Torres and Allan 2016). Thanks to their ability to potentiate cell therapy by being a marker of highly therapeutic MSCs, this family of cyto-protective enzymes is important to investigate. Complementary to our study, Vulcano and colleagues proved that WJ-MSCs induced lung cancer stem cell proliferation with higher ALDH⁺ cells depending tumor type, these results suggest that the effect of WJ-MSC could be influenced by several factors (Vulcano et al. 2016). In this work, thanks to Fluorescence Activated Cell Sorting (FACS), we sorted two subsets of WJ-MSCs based on their ALDH activity (reported as ALDH⁺ and ALDH⁻). By harboring specific biological functionalities such as tissue repair activities and hematopoietic reconstitution, several cell progenitors with high ALDH activity have been shown to be therapeutically relevant (Balber 2011). The global gene expression profiles of a variety of non-hematopoietic progenitors are likely to have an important impact on their properties as well as on their cellular therapeutic application (De Kock et al. 2012). Both populations of WJ-MSCs demonstrated a distinct transcriptome profile (related to their ALDH activity) for genes associated with MSC major properties (stemness, cell-cycle, proliferation, phenotype, response to hypoxia, angiogenesis, multilineage capacities, immunomodulation and hematopoiesis support) (Kang et al. 2016; Stanko et al. 2014; Dolatabadi et al. 2017; Heo et al. 2016; Torensma et al. 2013). These differences between WJ-MSC populations may indicate biological features with high specific therapeutic relevance.

About the stemness (Rasini et al. 2013), Nanog, Rex1 and OCT-4 were more expressed in ALDH⁺ WJ-MSCs compared to ALDH⁻ counterpart. Our results were in accordance with previous studies reporting that these three genes were expressed by WJ-MSCs (Beeravolu et al. 2017; Van Pham et al. 2016).

Regarding cell cycle, we observed significant differences about the expression of CCNA, CCNB, CCNE, CDC25A, FosB, CDK1, CDK2, pRB, p16, p21 and p53. All the targets were increased in ALDH⁺ cells compared to ALDH⁻ cells. As the use of MSC in regenerative medicine may require large scale expansion, it's thus specially interesting to evaluate proliferation capacity of WJ-MSCs. Literature reported that the growth rate of WJ-MSCs was superior compared to the BM-MSCs due to higher proliferation with an upregulation of CCNA, CCNB, CDC25A and p53 (Batsali et al. 2017). The proliferation of WJ-MSCs has been influenced by obstetric factors (Wajid et al. 2015), themselves influenced by the In vitro passage of cells (Avercenc-Leger et al. 2017). These studies indicated that obstetric factors have to be considered to improve WJ-MSC proliferation. According our results WJ-MSC ALDH⁺ cells seem to have more potential for proliferation, important aspect that should envisaged for therapeutic use. ALDH activity could influence the cell cycle and modulate properties of cellular population (Dolatabadi et al. 2017; Meng et al. 2014; Hegab et al. 2014). Mechanistically, ALDH throughout the catabolism of some endogenous substrates have the capacity to either stimulate or inhibit the expression of genes involved in cell cycle and therefore actively involved in controlling cell proliferation (Muzio et al. 2012).

The phenotype of a cellular product is an important issue for optimal cell-based therapy (New et al. 2015) and the phenotype of WJ-MSCs was often investigated (Van Pham et al. 2016; Walecka et al. 2017). Progenitors cells may display difference for CD54, 58, 106, 146 and CD200 depending of their origins (Najar et al. 2010a; Najar et al. 2012; Vishnubalaji et al. 2012; Huang et al. 2010). Here, we noticed a significant increased expression of CD54, 58, 106, 146 and CD200 in ALDH⁺ WJ-MSCs. The expression of CD54, CD58 and CD106, main cell adhesion molecules, were shown to be tissue dependent (Najar et al. 2010a; Mandelli et al. 1999; Baer 2014). Interestingly, cells enriched in CD54 (Espagnollet et al. 2017) and CD106 (Yang et al. 2013; Du et al. 2016a) were shown to harbor great immunosuppressive capacities as well as potent pro-angiogenic abilities. Progenitor cells with enrichment on CD200 may also display distinguished immunomodulation (Najar et al. 2012), regenerative (Wang et al. 2014) and osteogenesis (Pontikoglou et al. 2016).

potentialities. In the other hand, striking stemness, multilineage and immunomodulatory capacities were reported for CD146 enriched cells (Wu et al. 2016).

The efficacy of MSC therapy is notably limited by poor survival of transplanted cells that face difficult microenvironment with low oxygen concentration. The ability of cells to response to hypoxia is another important point to evaluate. WJ-MSCs have been previously proved to don't be affected by ischemia and they thus be considered as a promising source for clinical applications (Himal et al. 2017). In this work, we observed an increased expression of HIF1 α , HIF2 α and GLUT1 in ALDH⁺ population compared to ALDH⁻ cells suggesting higher adaptation capacity to hypoxic environment. Hypoxia-inducible factors (HIFs) in a cell-type-specific manner are suggested to control different cellular functions such as angiogenesis, stemness and inflammation (Nauta et al. 2014; Bartels et al. 2013; D'Ippolito et al. 2006; Ohnishi et al. 2007). Thus, ALDH expression is likely involved in MSC resistance to oxidative stress (Kusuma et al. 2017).

MSCs have been widely proven effective for therapeutic angiogenesis in ischemia animal models as well as clinical vascular diseases. However, heterogeneous proangiogenic properties of MSCs derived from different tissue origins have been described and these differences are likely linked to the environment (Du et al. 2016b). In this study, we observed an increased expression for angiogenic genes ANG1, ANG2, FLT1 and VEGF in ALDH⁺ WJ-MSCs. WJ-MSCs have been proved to possess pro angiogenic activity suggesting these cells as an attractive source for their use in tissue engineering (Arutyunyan et al. 2016; Edwards et al. 2014). Based on ALDH activity, as a part of their tissue repair and regenerative functions, subsets of MSCs according to their ALDH activity may promote angiogenesis by upregulating FLT1, CXCR4, and ANG2 (Pontikoglou et al. 2016; Nauta et al. 2014).

Homeostasis of the hematopoietic system is an important function enrolled by MSCs providing several factors [IL6, IL8, MMP2 and SCF (Fajardo-Orduna et al. 2015)] in the hematopoietic stem cell (HSC) niche. We highlighted that ALDH⁺ subsets of WJ-MSCs present a potent hematopoiesis-supporting capacity by the significant up-regulation of SCF, SDF1, IL6, IL8 and MMP2 gene expression. By increasing the expression of MMP-2, IL-6 and IL-8

were involved in supporting the engraftment and migration of repopulating cells within the bone marrow (Briquet et al. 2010).

According to their immunological properties, WJ-MSCs are likely valuable candidates for allogeneic therapy (El Omar et al. 2014). Indeed, MSCs present immunomodulatory functions and therefore regulate the biology of several immune cells (Lee et al. 2012; Rizk et al. 2017; Abdi et al. 2008; Najar et al. 2010b; Purandare et al. 2014). ALDH⁺ WJ-MSCs demonstrated increased expression of COX1-2, GAL1, LIF and HGF which indicate better immunomodulatory capacity and thus might be more attractive for immunotherapeutic interventions. These MSC derived factors are suggested to actively compete for the establishment of a tolerogenic state (Najar et al. 2016b). Accordingly, ALDH was shown to be critical for the induction of T-regs and thus promoting immunological tolerance (Steimle and Frick 2016).

We finally addressed the expression of the specific genes associated with their tri-lineage potential of MSCs (Rohban and Pieber 2017; Vella et al. 2011). Indeed, Wharton's jelly MSCs are endowed with high trilineage potential and thus are important for tissue repair and regeneration. In line with the results of (Zajdel et al. 2017), OSX, BSP, OPG, OPN and Runx2 were more expressed in ALDH⁺ cells suggesting that this population clearly owned more capacities to differentiate into osteoclasts than ALDH⁻ cells.

Concerning adipogenesis, Chen and colleagues showed that WJ-MSCs may differentiate into adipocytes and osteocytes (Chen et al. 2015). Counter that, Batsali and colleagues showed minor adipogenesis capacity in WJ-MSCs compared to BM-MSCs due to decreased expression of PPAR γ and CEBP α (Batsali et al. 2017). In our study, adipogenic markers CEBP α , CEBP δ , PPAR γ , KLF2, KLF5 (Menssen et al. 2011; Lee and Ge 2014; Su et al. 2017) were most expressed in ALDH⁺ WJ-MSCs.

We finally evaluated the potential differentiation capacity of WJ-MSCs into chondroblasts (Ronziere et al. 2010; Gonzalez-Fernandez et al. 2015). In this work, we demonstrated that ALDH⁺ subsets presented more expression of chondrogenic genes (Sox9, ACAM, COMP, COL2 α 1). The chondrogenesis has been largely reported as WJ-MSC capacity (Baksh et al. 2007; Reppel et al. 2015). The work of Aleksander-Konert and colleagues notably proved the capacity of WJ-MSCs in chondrogenesis

(Aleksander-Konert et al. 2016) although literature proved that ALDH activity is not relevant for chondrogenesis capacity of MSCs (Estes et al. 2006).

Based on these results, we proved that ALDH⁺ WJ-MSCs have more abilities to express pluripotent genes, to proliferate, to display potent immunomodulatory ability, to support hematopoiesis and angiogenesis, to response to hypoxia but also to differentiate into osteo-, chondro- and adipocyte-lineages compared to ALDH[−] population. This specific ALDH⁺ subpopulation thus appears to be useful in numerous clinical applications. In addition to being a pivotal marker for stem/progenitor cell populations, the use of ALDH allow to identify a subset of WJ-MSCs with specific gene features pointing out that targeted therapeutic application based on these findings is feasible.

Acknowledgements We thank “Télévie” (FNRS) for the financial support.

Authors’ contributions Conceived and designed the experiments: MN, LL. Performed the experiments: MN, LL. Analyzed the data: EC, MN, LD. Contributed reagents/materials/analysis tools: LD, LVG. Wrote the paper: EC, MN, LL.

Funding Mehdi Najar is awardee of a “Télévie” post-doctoral fellowship and Emerence Crompot is awardee of Ph.D. Grant “Télévie” (F.N.R.S.).

Compliance with ethical standards

Conflict of interest The authors declare that they have no conflict of interest.

Ethical standard This study was approved by the Bordet Institute Ethics Committee (Belgium) and conducted in accordance with the Declaration of Helsinki (1964). All donors and/or their parents gave written informed consent.

Availability of data and materials All data generated or analyzed during this study are included in this published article (and its supplementary information files).

References

- Abdi R, Fiorina P, Adra CN, Atkinson M, Sayegh MH (2008) Immunomodulation by mesenchymal stem cells: a potential therapeutic strategy for type 1 diabetes. *Diabetes* 57:1759–1767
- Aleksander-Konert E, Padaszynski P, Zajdel A, Dzierzewicz Z, Wilczok A (2016) In vitro chondrogenesis of Wharton’s jelly mesenchymal stem cells in hyaluronic acid-based hydrogels. *Cell Mol Biol Lett* 21:11
- Alison MR, Guppy NJ, Lim SML, Nicholson LJ (2010) Finding cancer stem cells: are aldehyde dehydrogenases fit for purpose? *J Pathol* 222:335–344
- Arutyunyan I, Elchaninov A, Makarov A, Fatkhudinov T (2016) Umbilical cord as prospective source for mesenchymal stem cell-based therapy. *Stem Cells Int* 2016:6901286
- Atouf F, Provost NM, Rosenthal FM (2013) Standards for ancillary materials used in cell- and tissue-based therapies. MBA Sunday, September 1, 2013. <http://www.bioprocessintl.com/upstream-processing/biochemicals-raw-materials/standards-for-ancillary-materials-used-in-cell-and-tissue-based-therapies-346300/>
- Avercenc-Leger L, Guerci P, Virion JM et al (2017) Umbilical cord-derived mesenchymal stromal cells: predictive obstetric factors for cell proliferation and chondrogenic differentiation. *Stem Cell Res Ther* 8:161
- Baer PC (2014) Adipose-derived mesenchymal stromal/stem cells: an update on their phenotype in vivo and in vitro. *World J Stem Cells* 6:256–265
- Baksh D, Yao R, Tuan RS (2007) Comparison of proliferative and multilineage differentiation potential of human mesenchymal stem cells derived from umbilical cord and bone marrow. *Stem Cells* 25:1384–1392
- Balber AE (2011) Concise review: aldehyde dehydrogenase bright stem and progenitor cell populations from normal tissues: characteristics, activities, and emerging uses in regenerative medicine. *Stem Cells* 29:570–575
- Bartels K, Grenz A, Eltzhischig HK (2013) Hypoxia and inflammation are two sides of the same coin. *Proc Natl Acad Sci USA* 110:18351–18352
- Batsali AK, Pontikoglou C, Koutroulakis D et al (2017) Differential expression of cell cycle and WNT pathway-related genes accounts for differences in the growth and differentiation potential of Wharton’s jelly and bone marrow-derived mesenchymal stem cells. *Stem Cell Res Ther* 8:102
- Beeravolu N, McKee C, Alamri A et al (2017) Isolation and characterization of mesenchymal stromal cells from human umbilical cord and fetal placenta. *J Vis Exp*. <https://doi.org/10.3791/55224>
- Boey PYK, Lim SLD, Tang KF et al (2017) Comparative study of the methods of extracting mesenchymal stem cells from cryopreserved Wharton’s jelly. *J Stem Cells Regen Med* 13:29–32
- Briquet A, Dubois S, Bekaert S et al (2010) Prolonged ex vivo culture of human bone marrow mesenchymal stem cells influences their supportive activity toward NOD/SCID-repopulating cells and committed progenitor cells of B lymphoid and myeloid lineages. *Haematologica* 95:47–56
- Busser H, Najar M, Raicevic G et al (2015) Isolation and characterization of human mesenchymal stromal cell subpopulations: comparison of bone marrow and adipose tissue. *Stem Cells Dev* 24:2142–2157
- Chen G, Yue A, Ruan Z et al (2015) Comparison of biological characteristics of mesenchymal stem cells derived from maternal-origin placenta and Wharton’s jelly. *Stem Cell Res Ther* 6:228
- Davies JE, Walker JT, Keating A (2017) Concise review: Wharton’s jelly: the rich, but enigmatic, source of

- mesenchymal stromal cells. *Stem Cells Transl Med* 6:1620–1630
- De Kock J, Najar M, Bolleyn J et al (2012) Mesoderm-derived stem cells: the link between the transcriptome and their differentiation potential. *Stem Cells Dev* 21:3309–3323
- D'Ippolito G, Diabira S, Howard GA, Roos BA, Schiller PC (2006) Low oxygen tension inhibits osteogenic differentiation and enhances stemness of human MIAMI cells. *Bone* 39:513–522
- Dolatabadi S, Candia J, Akrap N et al (2017) Cell cycle and cell size dependent gene expression reveals distinct subpopulations at single-cell level. *Front Genet* 8:1
- Dolle L, Best J, Empsen C et al (2012) Successful isolation of liver progenitor cells by aldehyde dehydrogenase activity in naive mice. *Hepatology* 55:540–552
- Dolle L, Boulter L, Leclercq IA, van Grunsven LA (2015) Next generation of ALDH substrates and their potential to study maturational lineage biology in stem and progenitor cells. *Am J Physiol Gastrointest Liver Physiol* 308:G573–G578
- Du W, Li X, Chi Y et al (2016a) VCAM-1 + placenta chorionic villi-derived mesenchymal stem cells display potent pro-angiogenic activity. *Stem Cell Res Ther* 7:49
- Du WJ, Chi Y, Yang ZX et al (2016b) Heterogeneity of proangiogenic features in mesenchymal stem cells derived from bone marrow, adipose tissue, umbilical cord, and placenta. *Stem Cell Res Ther* 7:163
- Dunavin N, Dias A, Li M, McGuirk J (2017) Mesenchymal stromal cells: What is the mechanism in acute graft-versus-host disease? *Biomedicine* 5:39
- Edwards SS, Zavala G, Prieto CP et al (2014) Functional analysis reveals angiogenic potential of human mesenchymal stem cells from Wharton's jelly in dermal regeneration. *Angiogenesis* 17:851–866
- El Omar R, Beroud J, Stoltz JF et al (2014) Umbilical cord mesenchymal stem cells: the new gold standard for mesenchymal stem cell-based therapies? *Tissue Eng B Rev* 20:523–544
- Espagnolle N, Balguerie A, Arnaud E, Sensebe L, Varin A (2017) CD54-mediated interaction with pro-inflammatory macrophages increases the immunosuppressive function of human mesenchymal stromal cells. *Stem Cell Rep* 8:961–976
- Estes BT, Wu AW, Storms RW, Guilak F (2006) Extended passaging, but not aldehyde dehydrogenase activity, increases the chondrogenic potential of human adipose-derived adult stem cells. *J Cell Physiol* 209:987–995
- Fajardo-Orduna GR, Mayani H, Montesinos JJ (2015) Hematopoietic support capacity of mesenchymal stem cells: biology and clinical potential. *Arch Med Res* 46:589–596
- Fayyad-Kazan M, Najar M, Fayyad-Kazan H, Raicevic G, Lagneaux L (2017) Identification and evaluation of new immunoregulatory genes in mesenchymal stromal cells of different origins: comparison of normal and inflammatory conditions. *Med Sci Monit Basic Res* 23:87–96
- Forostyak S, Jendelova P, Sykova E (2013) The role of mesenchymal stromal cells in spinal cord injury, regenerative medicine and possible clinical applications. *Biochimie* 95:2257–2270
- Gonzalez-Fernandez ML, Perez-Castrillo S, Ordas-Fernandez P et al (2015) Study on viability and chondrogenic differentiation of cryopreserved adipose tissue-derived mesenchymal stromal cells for future use in regenerative medicine. *Cryobiology* 71:256–263
- Hegab AE, Ha VL, Bisht B et al (2014) Aldehyde dehydrogenase activity enriches for proximal airway basal stem cells and promotes their proliferation. *Stem Cells Dev* 23:664–675
- Heo JS, Choi Y, Kim HS, Kim HO (2016) Comparison of molecular profiles of human mesenchymal stem cells derived from bone marrow, umbilical cord blood, placenta and adipose tissue. *Int J Mol Med* 37:115–125
- Herzenberg LA, Parks D, Sahaf B et al (2002) The history and future of the fluorescence activated cell sorter and flow cytometry: a view from Stanford. *Clin Chem* 48:1819–1827
- Himal I, Goyal U, Ta M (2017) Evaluating Wharton's jelly-derived mesenchymal stem cell's survival, migration, and expression of wound repair markers under conditions of ischemia-like stress. *Stem Cells Int* 2017:5259849
- Hoogduijn MJ, Popp F, Verbeek R et al (2010) The immunomodulatory properties of mesenchymal stem cells and their use for immunotherapy. *Int Immunopharmacol* 10:1496–1500
- Huang HI, Chen SK, Ling QD et al (2010) Multilineage differentiation potential of fibroblast-like stromal cells derived from human skin. *Tissue Eng A* 16:1491–1501
- Kamolz LP, Keck M, Kasper C (2014) Wharton's jelly mesenchymal stem cells promote wound healing and tissue regeneration. *Stem Cell Res Ther* 5:62
- Kang CM, Kim H, Song JS et al (2016) Genetic comparison of stemness of human umbilical cord and dental pulp. *Stem Cells Int* 2016:3453890
- Kusuma GD, Abumaree MH, Pertile MD et al (2016) Mesenchymal stem/stromal cells derived from a reproductive tissue niche under oxidative stress have high aldehyde dehydrogenase activity. *Stem Cell Rev* 12:285–297
- Kusuma GD, Abumaree MH, Perkins AV, Brennecke SP, Kalionis B (2017) Reduced aldehyde dehydrogenase expression in preeclamptic decidual mesenchymal stem/stromal cells is restored by aldehyde dehydrogenase agonists. *Sci Rep* 7:42397
- Lee JE, Ge K (2014) Transcriptional and epigenetic regulation of PPARgamma expression during adipogenesis. *Cell Biosci* 4:29
- Lee JM, Jung J, Lee HJ et al (2012) Comparison of immunomodulatory effects of placenta mesenchymal stem cells with bone marrow and adipose mesenchymal stem cells. *Int Immunopharmacol* 13:219–224
- Ma I, Allan AL (2011) The role of human aldehyde dehydrogenase in normal and cancer stem cells. *Stem Cell Rev* 7:292–306
- Mandelli F, Lauria F, Majolino I (1999) Autologous transplantation with peripheral blood stem cells in chronic lymphocytic leukemia. *Hematol Cell Ther* 41:117–125
- Meng E, Mitra A, Tripathi K et al (2014) ALDH1A1 maintains ovarian cancer stem cell-like properties by altered regulation of cell cycle checkpoint and DNA repair network signaling. *PLoS ONE* 9:e107142
- Menssen A, Haupl T, Sittinger M et al (2011) Differential gene expression profiling of human bone marrow-derived

- mesenchymal stem cells during adipogenic development. *BMC. Genomics* 12:461
- Moreb JS, Ucar D, Han S et al (2012) The enzymatic activity of human aldehyde dehydrogenases 1A2 and 2 (ALDH1A2 and ALDH2) is detected by Aldefluor, inhibited by diethylaminobenzaldehyde and has significant effects on cell proliferation and drug resistance. *Chem Biol Interact* 195:52–60
- Muzio G, Maggiora M, Paiuzzi E, Oraldi M, Canuto RA (2012) Aldehyde dehydrogenases and cell proliferation. *Free Radic Biol Med* 52:735–746
- Nagamura-Inoue T, He H (2014) Umbilical cord-derived mesenchymal stem cells: their advantages and potential clinical utility. *World J Stem Cells* 6:195–202
- Najar M, Raicevic G, Boufker HI et al (2010a) Mesenchymal stromal cells use PGE2 to modulate activation and proliferation of lymphocyte subsets: combined comparison of adipose tissue, Wharton's jelly and bone marrow sources. *Cell Immunol* 264:171–179
- Najar M, Raicevic G, Id Boufker H et al (2010b) Modulated expression of adhesion molecules and galectin-1: role during mesenchymal stromal cell immunoregulatory functions. *Exp Hematol* 38:922–932
- Najar M, Raicevic G, Jebbawi F et al (2012) Characterization and functionality of the CD200-CD200R system during mesenchymal stromal cell interactions with T-lymphocytes. *Immunol Lett* 146:50–56
- Najar M, Raicevic G, Fayyad-Kazan H et al (2015) Bone marrow mesenchymal stromal cells induce proliferative, cytokinic and molecular changes during the T cell response: the importance of the IL-10/CD210 axis. *Stem Cell Rev* 11:442–452
- Najar M, Raicevic G, Andre T et al (2016a) Mesenchymal stromal cells from the foreskin: tissue isolation, cell characterization and immunobiological properties. *Cytotherapy* 18:320–335
- Najar M, Raicevic G, Crompton E et al (2016b) The immunomodulatory potential of mesenchymal stromal cells: a story of a regulatory network. *J Immunother* 39:45–59
- Nauta TD, van Hinsbergh VWM, Koolwijk P (2014) Hypoxic signaling during tissue repair and regenerative medicine. *Int J Mol Sci* 15:19791–19815
- New SEP, Alvarez-Gonzalez C, Vagaska B et al (2015) A matter of identity—phenotype and differentiation potential of human somatic stem cells. *Stem Cell Res* 15:1–13
- Ohnishi S, Yasuda T, Kitamura S, Nagaya N (2007) Effect of hypoxia on gene expression of bone marrow-derived mesenchymal stem cells and mononuclear cells. *Stem Cells* 25:1166–1177
- Pontikoglou C, Langonne A, Ba MA et al (2016) CD200 expression in human cultured bone marrow mesenchymal stem cells is induced by pro-osteogenic and pro-inflammatory cues. *J Cell Mol Med* 20:655–665
- Purandare B, Teklemariam T, Zhao L, Hantash BM (2014) Temporal HLA profiling and immunomodulatory effects of human adult bone marrow- and adipose-derived mesenchymal stem cells. *Regen Med* 9:67–79
- Rasini V, Dominici M, Kluba T et al (2013) Mesenchymal stromal/stem cells markers in the human bone marrow. *Cytotherapy* 15:292–306
- Reppel L, Schiavi J, Charif N et al (2015) Chondrogenic induction of mesenchymal stromal/stem cells from Wharton's jelly embedded in alginate hydrogel and without added growth factor: an alternative stem cell source for cartilage tissue engineering. *Stem Cell Res Ther* 6:260
- Rizk M, Aziz J, Shorr R, Allan DS (2017) Cell-based therapy using umbilical cord blood for novel indications in regenerative therapy and immune modulation: an updated systematic scoping review of the literature. *Biol Blood Marrow Transplant* 23:1607–1613
- Rodriguez-Torres M, Allan AL (2016) Aldehyde dehydrogenase as a marker and functional mediator of metastasis in solid tumors. *Clin Exp Metastasis* 33:97–113
- Rohban R, Pieber TR (2017) Mesenchymal stem and progenitor cells in regeneration: tissue specificity and regenerative potential. *Stem Cells Int* 2017:5173732
- Ronzieri MC, Perrier E, Mallein-Gerin F, Freyria AM (2010) Chondrogenic potential of bone marrow- and adipose tissue-derived adult human mesenchymal stem cells. *Biomed Mater Eng* 20:145–158
- Sharpe ME, Morton D, Rossi A (2012) Nonclinical safety strategies for stem cell therapies. *Toxicol Appl Pharmacol* 262:223–231
- Sherman SE, Kuljanin M, Cooper TT et al (2017) High aldehyde dehydrogenase activity identifies a subset of human mesenchymal stromal cells with vascular regenerative potential. *Stem Cells* 35:1542–1553
- Stanko P, Kaiserova K, Altanerova V, Altaner C (2014) Comparison of human mesenchymal stem cells derived from dental pulp, bone marrow, adipose tissue, and umbilical cord tissue by gene expression. *Biomed Pap Med Fac Univ Palacky Olomouc Czech Repub* 158:373–377
- Steimle A, Frick JS (2016) Molecular mechanisms of induction of tolerant and tolerogenic intestinal dendritic cells in mice. *J Immunol Res* 2016:1958650
- Storms RW, Trujillo AP, Springer JB et al (1999) Isolation of primitive human hematopoietic progenitors on the basis of aldehyde dehydrogenase activity. *Proc Natl Acad Sci USA* 96:9118–9123
- Su Y, Shen X, Chen J et al (2017) Differentially expressed genes in PPARGgamma-deficient MSCs. *Mol Cell Endocrinol*
- Torensma R, Prins HJ, Schrama E et al (2013) The impact of cell source, culture methodology, culture location, and individual donors on gene expression profiles of bone marrow-derived and adipose-derived stromal cells. *Stem Cells Dev* 22:1086–1096
- Van Pham P, Truong NC, Le PT-B et al (2016) Isolation and proliferation of umbilical cord tissue derived mesenchymal stem cells for clinical applications. *Cell Tissue Bank* 17:289–302
- Vella JB, Thompson SD, Bucsek MJ, Song M, Huard J (2011) Murine and human myogenic cells identified by elevated aldehyde dehydrogenase activity: implications for muscle regeneration and repair. *PLoS ONE* 6:e29226
- Vishnubalaji R, Manikandan M, Al-Nbaheen M et al (2012) In vitro differentiation of human skin-derived multipotent stromal cells into putative endothelial-like cells. *BMC Dev Biol* 12:7
- Vulcano F, Milazzo L, Ciccarelli C et al (2016) Wharton's jelly mesenchymal stromal cells have contrasting effects on proliferation and phenotype of cancer stem cells from

- different subtypes of lung cancer. *Exp Cell Res* 345:190–198
- Wajid N, Naseem R, Anwar SS et al (2015) The effect of gestational diabetes on proliferation capacity and viability of human umbilical cord-derived stromal cells. *Cell Tissue Bank* 16:389–397
- Walecka I, Gil-Kulik P, Krzyzanowski A et al (2017) Phenotypic characterization of adherent cells population CD34 + CD90 + CD105 + derived from Wharton's jelly. *Med Sci Monit* 23:1886–1895
- Wang J, Zhu Z, Huang Y et al (2014) The subtype CD200-positive, chorionic mesenchymal stem cells from the placenta promote regeneration of human hepatocytes. *Biotechnol Lett* 36:1335–1341
- Wu CC, Liu FL, Sytwu HK, Tsai CY, Chang DM (2016) CD146 + mesenchymal stem cells display greater therapeutic potential than CD146-cells for treating collagen-induced arthritis in mice. *Stem Cell Res Ther* 7:23
- Yang ZX, Han ZB, Ji YR et al (2013) CD106 identifies a subpopulation of mesenchymal stem cells with unique immunomodulatory properties. *PLoS ONE* 8:e59354
- Zajdel A, Kalucka M, Kokoszka-Mikolaj E, Wilczok A (2017) Osteogenic differentiation of human mesenchymal stem cells from adipose tissue and Wharton's jelly of the umbilical cord. *Acta Biochim Pol* 64:365–369
- Zimmerlin L, Park TS, Zambidis ET, Donnenberg VS, Donnenberg AD (2013) Mesenchymal stem cell secretome and regenerative therapy after cancer. *Biochimie* 95:2235–2245